Research of Pattern Formation, edited by R. Takaki, pp. 517–535.

Stereology on Crack Geometry

Masanobu ODA

Department of Foundation Engineering, Faculty of Engineering, Saitama University, Urawa, Saitama 338, Japan

Abstract. Crack geometry, which is closely related to the mechanical anisotropy of discontinuous materials like rocks and rock masses, can be concisely expressed by a tensor (called the crack tensor) introduced by Oda. In this paper, an actual rock mass is studied to see if the crack tensor can be actually determined in situ. It is proved that stereology, based on geometrical statistics, provides a sound basis for determining the crack tensor.

1. Introduction

Rock masses are seldom free from geological discontinuities such as joints and faults. The network of joints usually exhibits very complicated geometry and varies, depending on the geological setting, from one place to another. In order to describe such jointed rock masses concisely, we need a simple, but still general, descriptive measure for the geometry. Such a measure, if we have, will lead rock engineers to better understanding of the mechanical properties of jointed rock masses, and will help them at least with choosing the proper values of hydromechanical constants by taking account of the effect of the joint geometry more explicitly.

Extensive works have been done to search a proper measure of the joint geometry through which we can access to the deformability and permeability of jointed rock masses. The research has not been completed yet, but rather we can say that there are still a lot of works to be done. However, some progress has been achieved recently. Here, we will review briefly some of the recent progress, with special emphasis on the use of stereology.

2. Fundamentals of Rock Joints

No geological body is homogeneous in the strict sense. However, it can be divided into statistically homogeneous domains each of which appears homogeneous at some macro-scale.

We will start our discussion with describing briefly fundamental elements of joints in each homogeneous domain; i.e., orientation, size, density and aperture of joints. Note, however, that our purpose is not to try to give the complete description, but is rather restricted to what we need in the subsequent paragraphs.

Volume density: Position of joints can be recognized by their centers. Let $m^{(V)}$ be the number of the centers in volume V. The volume density of joints ρ is defined by

$$\rho = \frac{m^{(V)}}{V} \tag{1}$$

Orientation of joints: Each joint consists of two parallel surfaces, the direction of each being characterized by an outward unit normal vector. Accordingly, two unit vectors $\boldsymbol{n}^{(+)}$ and $\boldsymbol{n}^{(-)}$ are assigned to each joint, so that $2m^{(V)}$ is the total number of joint surfaces in the volume V. For simplicity, these two vectors are both denoted by $\boldsymbol{n}$. Let $d\Omega$ be a small solid angle. Then, a density function $E(\boldsymbol{n})$ is introduced such that $2m^{(V)}E(\boldsymbol{n})d\Omega$ gives the number of joint surfaces (also equal to the number of joints) whose unit normal vectors are oriented within the small solid angle $d\Omega$. The density function must satisfy the following condition:

$$\int_{\Omega} E(\boldsymbol{n})d\Omega = 2\int_{\Omega/2} E(\boldsymbol{n})d\Omega \tag{2}$$

where Ω and $\Omega/2$ are solid angles indicating the limits of integration; that is, $\Omega(=4\pi)$ is for an entire unit sphere while $\Omega/2(=2\pi)$ is for unit hemisphere. Since $E(\boldsymbol{n}) = E(-\boldsymbol{n})$, the integration of $E(\boldsymbol{n})d\Omega$ over Ω has the same value as that of $2E(\boldsymbol{n})d\Omega$ over $\Omega/2$. This rule is also applicable to the integration of $P(\boldsymbol{n})E(\boldsymbol{n})d\Omega$ as long as $P(\boldsymbol{n})$ equals $P(-\boldsymbol{n})$.

Orientation of joints is recorded by measuring their dips and strikes, and is reported as a cluster of poles on Schmidt's equal area net. Contour lines are sometimes constructed to show the percentage concentration of $\boldsymbol{n}$ per unit percent area. It is easy to prove that the percentage of each contour line, if it is divided by 4π, has exactly the same meaning as the contour value of $E(\boldsymbol{n})$ (Oda, 1985). Making such a contour diagram is so common that $E(\boldsymbol{n})$ can be regarded as a known function. In order to determine a reliable function of $E(\boldsymbol{n})$, of course, special care is needed to avoid biased sampling of joints.

Size of joints: It is difficult to say much about joint size since exact information

on the shape of joints is so limited. Diameter r, with the following definition, is tentatively used as an index of the joint size: Consider a flat joint with area S and substitute an equivalent circle of diameter r for it; i.e., $r = 2(S/\pi)^{1/2}$.

A density function $f(r)$ is introduced such that $f(r)dr$ gives the probability of joints whose size range is within r to $r + dr$. No information is available to say more about $f(r)$. We can use, if necessary, an exponential function given by

$$f(r) = \lambda \exp(-\lambda r) \tag{3}$$

It is the simplest function with the mean and standard deviation both equal to $1/\lambda$.

A density function $E(\boldsymbol{n}, r)$ must be used in more general cases in which $\boldsymbol{n}$ is not statistically independent of r. If they are independent, $E(\boldsymbol{n}, r)$ equals $E(\boldsymbol{n})f(r)$.

Aperture: Aperture is one of the most important aspects of a joint. A joint is sometimes modeled as a set of parallel plates with aperture t. Recent studies have shown that such a parallel plate model oversimplifies the reality of joints. Complicated structure is commonly observed inside a joint, and is never specified by a unique value of the aperture. In the theoretical study, however, only the parallel plate can be an amenable model of a joint.

3. Index Measure for Joint Geometry

In the study of granular mechanics, several tensors were introduced to characterize anisotropic geometry produced by discrete particles (Satake, 1983; Kanatani, 1984). Among them, a tensor defined by

$$N_{ij} = \int_{\Omega} n_i n_j E(\boldsymbol{n}) d\Omega \tag{4}$$

is also useful if n_i ($i = 1, 2, 3$) are read as components of a unit normal vector $\boldsymbol{n}$ with respect to orthogonal reference axes x_i ($i = 1, 2, 3$). The subscripts i and j can be set to 1, 2 or 3. For example, n_1 is the direction cosine of $\boldsymbol{n}$ with respect to a reference axis x_1.

Note that the definition of N_{ij} is only concerned with the orientation of joints, without making any reference to the size as well as the density of joints. Kachanov (1980) introduced a tensor α_{ij} to quantify the geometry of micro-cracks in rocks:

$$\alpha_{ij} = (1/V) \sum_{k=1}^{m^{(V)}} \left(S^{(k)} \right)^{3/2} n_i^{(k)} n_j^{(k)} \tag{5}$$

where $S^{(k)}$ is the area of a kth micro-crack and $m^{(V)}$ is the number of micro-cracks in the related volume V. In this equation, the size as well as the number of micro-

cracks are taken into account in addition to their directions.

Kawamoto *et al.* (1988) regarded joints as damages, and defined a tensor Ω_{ij} called the damage tensor:

$$\Omega_{ij} = \left(\hat{l} / V\right) \sum_{k=1}^{m^{(V)}} S^{(k)} n_i^{(k)} n_j^{(k)} \tag{6}$$

where $\hat{l}$ is a characteristic length for a given system. Using the damage tensor, the conventional stress tensor is modified to yield a new stress measure. That is, damages cannot bear any stress along them so that solid matrix including damages must transfer higher stress than that free from damage.

Oda (1984) has also proposed a tensor $\boldsymbol{F}$ with components of $F_{ij\cdots k}$ (called the crack tensor);

$$F_{ij\cdots k} = \rho \int_0^\infty \int_0^\infty \int_\Omega S r n_i n_j \cdots n_k E(\boldsymbol{n}, r, S) d\Omega dr dS \tag{7}$$

Equation (7) is given in integral form since it can be easily handled in theoretical consideration. If necessary, however, the integral form can be substituted by the following additive one;

$$F_{ij\cdots l} = (1 / V) \sum_{k=1}^{m^{(V)}} S^{(k)} r^{(k)} n_i^{(k)} n_j^{(k)} \cdots n_i^{(k)} \tag{8}$$

The tensor has non-zero components only when the rank, which is equivalent to the number of subscripts of $F_{ij\cdots k}$, is even. This is because $E(\boldsymbol{n}, r) = E(-\boldsymbol{n}, r)$ due to symmetry. The component remains unchanged even if any pair of the subscripts is exchanged; i.e. $F_{ij\cdots k} = F_{ji\cdots k} = \ldots = F_{kj\cdots i}$. A contraction with respect to any pair of subscripts reduces its rank by 2. The contraction of $n_i n_j n_k n_l$ over $i = j$, for example, yields $n_k n_l$ since $n_i n_i = {n_1}^2 + {n_2}^2 = {n_3}^2 = 1$. (Here, the summation convention is used. That is, the summation is taken if any subscript appears twice like $n_i n_i$.) The zero-, second- and fourth-rank tensors are given as follows (Oda, 1984);
Zero-rank:

$$F_0 = (\pi\rho / 4) \int_0^\infty r^3 f(r) dr \tag{9}$$

Second-rank

$$F_{ij} = (\pi\rho / 4) \int_0^\infty \int_\Omega r^3 n_i n_j E(\boldsymbol{n}, r) d\Omega dr \tag{10}$$

Fourth-rank:

$$F_{ijkl} = (\pi\rho / 4)\int_0^\infty \int_\Omega r^3 n_i n_j n_k n_l E(\boldsymbol{n}, r) d\Omega dr \tag{11}$$

where S is equal to $(1/4)\pi r^2$ since each joint with S is replaced by an equivalent circle with diameter r. In the case that the related volume is limited, of course, the infinity limit in the integration of r must be replaced by the maximum size joints r_m. (Since $S^{3/2}$ equals $(\pi/4)^{3/2} r^3$, the second-rank tensor or Eq. (10) is essentially the same as the tensor α_{ij} proposed by Kachanov (Eq. (5).)

The tensors from Eqs. (4) to (11) are all dimensionless without making any reference to aperture t of joints. Oda *et al.* (1987) discussed a permeability tensor for hydraulically equivalent jointed rock masses, and found that a tensor P_{ij} with dimension of squared length is important:

$$P_{ij} = (\pi\rho / 4)\int_0^\infty \int_0^\infty \int_\Omega r^2 t^3 n_i n_j E(\boldsymbol{n}, r, t) d\Omega dr dt \tag{12}$$

Several tensors are available for use in practice for characterizing the joint geometry. Rock engineers may ask what is the purpose of introducing such tensors in rock mechanics. To demonstrate the merits of using them, the geometrical implication of the crack tensor is discussed in some more detail.

On the assumption that joint aperture increases in proportion to joint size, it can be proved that the zero-rank tensor F_0 holds an equivalent meaning to the porosity associated with joints (Oda, 1988). (Let us compare two samples having the same zero-rank tensor (=porosity). It is easy to understand that they are not necessarily the same with respect to the joint geometry. In order to differentiate them, we need higher rank tensors as will be discussed next.)

Since F_{ij} is a symmetric second-rank tensor just like a stress tensor, we can always find three principal values F_1, F_2 and F_3 in three directions called the principal axes. These axes, which are also the principal axes of anisotropy, are orthogonal even though non-orthogonal joint sets are concerned.

Consider a space whose axes are taken as F_1, F_2 and F_3 (Fig. 1). In this space, any crack tensor is expressed by a vector OP with the components of the corresponding principal values; i.e., $(\vec{OP})^T = (F_1, F_2, F_3)$. If $\vec{OP}$ is on the diagonal, the second-rank tensor is isotropic. The vector $\vec{OP}$ is decomposed into two components; i.e. $\vec{OP} = \vec{OA} + \vec{OB}$. The length of $\vec{OA}$ is related to the isotropic component while the length of $\vec{OB}$ the deviatoric (anisotropic) one. Accordingly, it can be said that the length of the vector $\vec{OB}$, if it is normalized by the length of the vector $\vec{OA}$, provides a reasonable measure for the anisotropy of joint geometry.

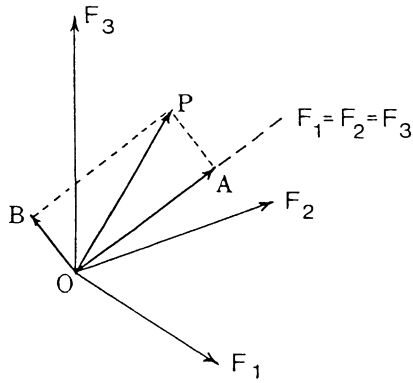

Fig. 1. Crack tensor in geometrical space. (The axes are taken as the principal values of crack tensor F_1, F_2 and F_3. The broken line is parallel to the space diagonal satisfying $F_1 = F_2 = F_3$.)

Two-dimensional joints are illustrated in squares of size a (depth T) in Fig. 2 whose abscissa and ordinate are parallel to the reference axes x_1 and x_2, respectively (Oda *et al.*, 1986). Let $\theta^{(k)}$ be the inclination angle of $\boldsymbol{n}^{(k)}$ (i.e., a unit vector normal to the kth joint) to the x_1-axis, and r and T be the joint length and the joint depth, respectively. Note that, for such two-dimensional cases, the direction cosine n_1 is given by $\cos\theta^{(k)}$ and n_2 by $\sin\theta^{(k)}$. The two-dimensional component of the crack tensor, for example F_{1122}, is calculated by

$$F_{1122} = \left(1/a^2T\right)\sum_{k=1}^{m^{(V)}} T\left(r^{(k)}\right)^2 \cos^2\theta^{(k)}\sin^2\theta^{(k)} \tag{13}$$

where a^2T stands for the volume V and $Tr^{(k)}$ for the surface area of kth joint in Eq. (8).

Sample (A): Sixteen joints with the same joint length of $r/a = 0.25$ are inserted. Half of them are oriented at $\theta = 0^\circ$, and the remainder at $\theta = 90^\circ$. The crack tensor is given in matrix form:

$$F_0^{(A)} = 1$$

$$F_{ij}^{(A)} = \begin{pmatrix} F_{11} & F_{12} \\ F_{21} & F_{22} \end{pmatrix} = \begin{pmatrix} 0.5 & 0 \\ 0 & 0.5 \end{pmatrix} \tag{14}$$

$$F_{ijkl}^{(A)} = \begin{pmatrix} F_{1111} & F_{1122} & F_{1112} \\ F_{2212} & F_{2222} & F_{2212} \\ F_{1211} & F_{1222} & F_{1212} \end{pmatrix} = \begin{pmatrix} 0.5 & 0 & 0 \\ 0 & 0.5 & 0 \\ 0 & 0 & 0 \end{pmatrix}$$

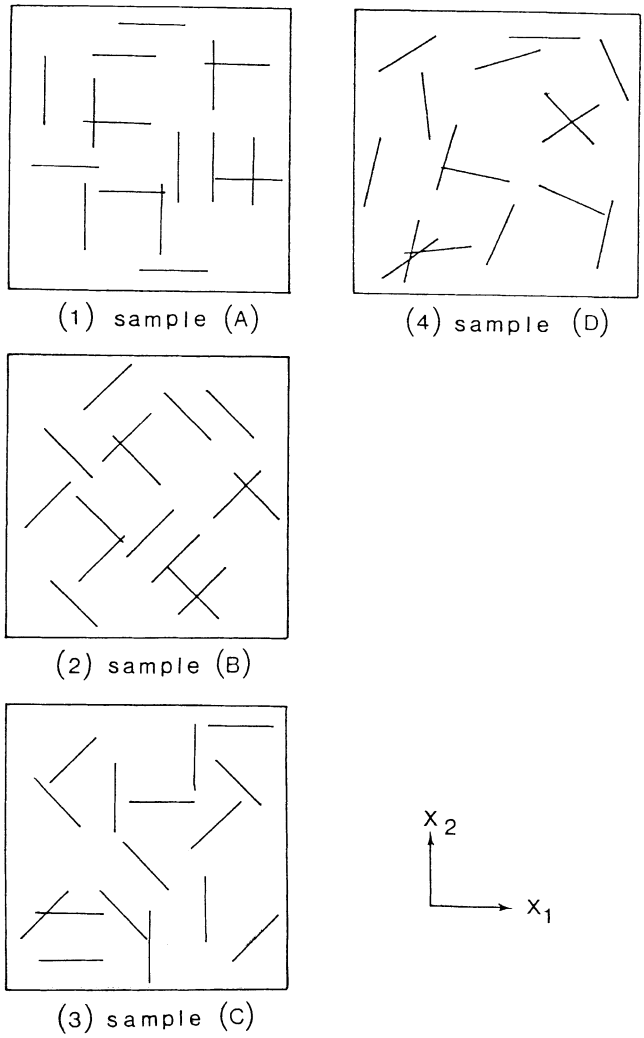

Fig. 2. Two-dimensional joint models. (The crack tensors in the text are calculated in reference to the given axes x_1 and x_2.)

Sample (B): Sample (B) is exactly the same as sample (A) except that all joints are rigidly rotated by 45° clockwise. The crack tensor is

$$F_0^{(B)} = 1$$

$$F_{ij}^{(B)} = \begin{pmatrix} 0.5 & 0 \\ 0 & 0.5 \end{pmatrix} \tag{15}$$

$$F_{ijkl}^{(B)} = \begin{pmatrix} 0.25 & 0.25 & 0 \\ 0.25 & 0.25 & 0 \\ 0 & 0 & 0.25 \end{pmatrix}$$

The second-rank tensor of sample (B) has the same non zero diagonals as those of sample (A). The tensor remains unchanged even after the sample is rotated. It can be easily checked that any rotation gives no effect on the components of the second-rank tensor. In this sense, the second-rank tensor is isotropic. The fourth-rank tensor of sample (B), on the other hand, is different from that of sample (A). Since the components depend on the choice of reference axes, it cannot be said to be isotropic any longer.

Sample (C): Sixteen joints are inserted at $\theta = 0°, 45°, 90°$ and $135°$, four joints for each orientation. The crack tensor is given by

$$F_0^{(C)} = 1$$

$$F_{ij}^{(C)} = \begin{pmatrix} 0.5 & 0 \\ 0 & 0.5 \end{pmatrix} \tag{16}$$

$$F_{ijkl}^{(C)} = \begin{pmatrix} 0.375 & 0.125 & 0 \\ 0.125 & 0.375 & 0 \\ 0 & 0 & 0.125 \end{pmatrix}$$

Not only the second-rank tensor but also the fourth-rank tensor are both isotropic. We can easily ascertain that these components remain unchanged even if any rotation of the reference axes is given. However, the isotropy is lost when the sixth-rank tensor is introduced. In order to make the sample still isotropic in the sixth-rank tensor, an equal number of joints must be inserted at $\theta = 0°, 30°, 60°, 90°, 120°$ and $150°$, individually.

Sample (D): Orientation of joints is chosen as random as possible to make an isotropic sample. The crack tensor becomes

$$F_0^{(D)} = 1$$

$$F_{ij}^{(D)} = \begin{pmatrix} 0.488 & -0.09 \\ -0.09 & 0.512 \end{pmatrix} \tag{17}$$

$$F_{ijkl}^{(D)} = \begin{pmatrix} 0.378 & 0.109 & -0.039 \\ 0.109 & 0.403 & -0.056 \\ -0.039 & -0.056 & 0.109 \end{pmatrix}$$

Note that slight deviation from isotropy appears in the second- and fourth-rank tensors. The deviation comes from the random choice of joint orientation. There is no doubt, however, that such deviation may become unimportant by increasing the number of joints.

The above examples strongly suggest that the detail of the joint geometry is materialized only in higher rank tensors. The density function $E(\boldsymbol{n})$ can be written in a polynomial expression using either a spherical harmonic expansion in three-dimensional cases or Fourier series expansion in two-dimensional cases. According to Kanatani (1984), the higher order coefficients can be expressed in terms of the higher rank tensors. This supports our observation that the details of joint geometry can be expressed by the higher rank tensors.

4. Determination of Crack Tensor

The next problem to be solved is whether there is a reliable method to measure the tensors by using in situ data. There is no difficulty, of course, if all the information concerning joints is available (see Fig. 2). Since this is not usually the case in practice, we must show a general method which makes it possible to predict the tensors using the data obtained from field survey. To this end, we will discuss it on the basis of stereology (Oda, 1983). (All calculations will be done under the assumption that the random variables $\boldsymbol{n}$ and r are statistically independent of one another; i.e. $E(\boldsymbol{n}, r) = E(\boldsymbol{n})f(r)$. If this does not hold, joints are classified into a few groups for each of which the independency does hold. Then, the crack tensors are calculated individually, and are summed afterward.)

4.1 Number of joints crossed by scanning line

A straight scanning line ab of length h is introduced parallel to a unit vector $\boldsymbol{q}$ (Fig. 3). For a moment, our attention is concentrated on specific joints, which will be called the $(\boldsymbol{n}, r)$-joints. That is, they have unit normal vectors oriented inside a small solid angle $d\Omega$ around $\boldsymbol{n}$ and, at the same time, have diameters ranging from r to $r + dr$. Solid lines in Fig. 3 show a column whose central axis coincides with the scanning line ab. The cap and the bottom consist of the $(\boldsymbol{n}, r)$-joints so that the cross section has the area of an $(\boldsymbol{n}, r)$-joint projected on the plane perpendicular to $\boldsymbol{q}$; that is, $(1/4)\pi r^2 |\boldsymbol{n}\cdot\boldsymbol{q}|$. Here, the dot between $\boldsymbol{n}$ and $\boldsymbol{q}$ denotes the inner product, and $|\ |$ denotes the sign of absolute value.

Now suppose that the length of the column is so long that the volume V_0 is large enough. Importance of the volume arises from the fact that the $(\boldsymbol{n}, r)$-joints intersect

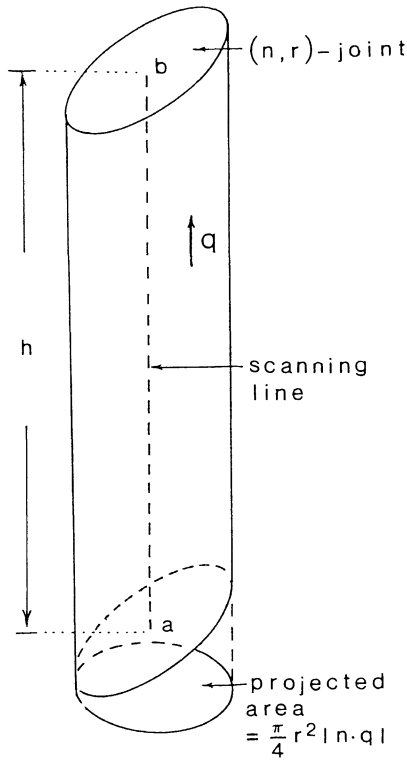

Fig. 3. Scanning line and its associated column. (Note that $(\boldsymbol{n}, f)$-joints intersect the scanning line ab if their centers are placed inside the column.)

the scanning line if their centers are located inside the volume. In other words, the number of the centers of $(\boldsymbol{n}, r)$-joints equals the number crossed by the scanning line.

The number of all joints $m^{(V_0)}$ involved in V_0, according to Eq. (1), can be estimated by

$$m^{(V_0)} = \rho V_0 = (1/4)\pi h \rho r^2 |\boldsymbol{n} \cdot \boldsymbol{q}| \tag{18}$$

Remember that $2E(\boldsymbol{n}, r)d\Omega dr$ stands for the probability of $(\boldsymbol{n}, r)$-joints. If $m^{(V_0)}$ is further multiplied by the probability, the number of $(\boldsymbol{n}, r)$-joints $dm^{(L)}$ whose centers are placed inside the column is calculated by

$$dm^{(L)} = (1/4)\pi h \rho r^2 |\boldsymbol{n} \cdot \boldsymbol{q}| 2E(\boldsymbol{n}, r)d\Omega dr \tag{19}$$

In order to count all joints (not restricted to the $(\boldsymbol{n}, r)$-joints) crossed by the scanning line of the length h, Eq. (19) must be integrated over $\Omega/2$ and $0 \le r \le \infty$. By dividing both sides by h, we have

$$\begin{aligned} m^{(L)} / h &= (1/4)\pi\rho \int_0^\infty r^2 f(r) \int_\Omega |\boldsymbol{n} \cdot \boldsymbol{q}| E(\boldsymbol{n}) d\Omega \\ &= (1/4)\pi\rho \langle r^2 \rangle \langle |\boldsymbol{n} \cdot \boldsymbol{q}| \rangle \end{aligned} \tag{20}$$

where

$$\langle r^2 \rangle = \int_0^\infty r^2 f(r) dr \tag{21}$$

$$\langle |\boldsymbol{n} \cdot \boldsymbol{q}| \rangle = \int_\Omega |\boldsymbol{n} \cdot \boldsymbol{q}| E(\boldsymbol{n}) d\Omega \tag{22}$$

where $\boldsymbol{n}$ is assumed to be statistically independent of r. It should be noted that $m^{(L)}/h$ is the number of joints crossed by unit length of the scanning line in the direction $\boldsymbol{q}$, and that it is sometimes counted in the conventional field survey. Also, $<|\boldsymbol{n}\cdot\boldsymbol{q}|>$ can be easily calculated using the additive form corresponding to Eq. (22) whenever the unit vectors normal to joints are given by poles of Schmidt net.

4.2 Number of joints crossed by excavated wall

Consider a plane, called the x_i-plane, which is normal to an x_i-axis. The plane just corresponds to an excavated wall (or a cliff) in a rock mass. Some joints are visible as lines (called traces) on the x_i-plane only if they intersect it. First consider an $(\boldsymbol{n}, r)$-joint in Fig. 4, and let z be the distance between the center of the joint and the plane. The joint will be tangent to the x_i-plane at P if z equals $(r/2)(1-n_i^2)^{1/2}$. The parallelogram drawn in Fig. 4 by broken lines has the following characteristics: 1) Its side planes (efgh and ijkl) are parallel to the x_i-plane. 2) Its upper and lower planes (eilh and fjkg) are parallel to the $(\boldsymbol{n}, r)$-joints.

If the area of the x_i-plane is equal to a^2, the volume V_0 of the parallelogram becomes $a^2 r(1-n_i^2)^{1/2}$. If the centers of the $(\boldsymbol{n}, r)$-joints are placed inside the parallelogram, they must intersect the x_i-plane and make traces with lengths ranging from 0 to r. (If an $(\boldsymbol{n}, r)$-joint is placed at the distance of $(r/2)(1-n_i^2)^{1/2}$, the trace length shrinks to zero. If the center is just on the plane, then the trace length equals the diameter r.) In a similar way of getting Eq. (19), the number $dM^{(i)}$ of the $(\boldsymbol{n}, r)$-joints making these traces is given by

$$\begin{aligned} dM^{(i)} &= \rho V_0 2E(\boldsymbol{n}) f(r) d\Omega dr \\ &= \rho a^2 r \left(1 - n_i^2\right)^{1/2} 2E(\boldsymbol{n}) f(r) d\Omega dr \end{aligned} \tag{23}$$

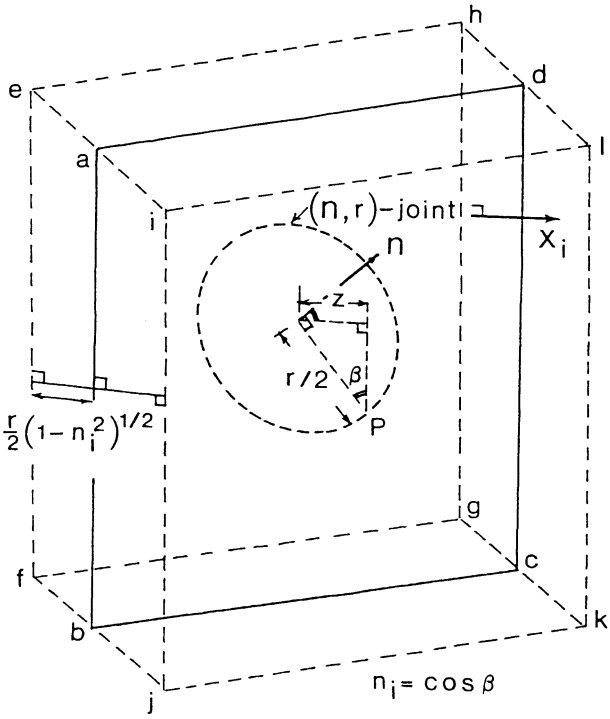

Fig. 4. Excavated wall (abcd) and its associated parallelogram (efghijkl). (Note that($\boldsymbol{n}, r$)-joints intersect the excavated wall to make traces if their centers are placed inside the parallelogram.)

Only the ($\boldsymbol{n}$, r)-joints are considered in this equation. In order to count all joints intersecting the x_i-plane, Eq. (23) must be integrated over $\Omega/2$ and $0 \leq r < \infty$ as follows:

$$M^{(i)} = 2a^2\rho\int_0^{\infty}\int_{\Omega/2} r\left(1-n_i^2\right)^{1/2} E(\boldsymbol{n})f(r)d\Omega dr \tag{24}$$

Now, a new density function $E^{(i)}(\boldsymbol{n}, r)$ is introduced such that $E^{(i)}(\boldsymbol{n}, r)d\Omega dr$ gives the probability of the ($\boldsymbol{n}, r$)-joints visible on the x_i-plane. Then, $E^{(i)}(\boldsymbol{n}, r)$ is the density function under the condition that we are only concerned with the joints intersecting the x_i-plane. Since $M^{(i)}E^{(i)}(\boldsymbol{n}, r)d\Omega dr$ equals $dM^{(i)}$, we have

$$E^{(i)}(\boldsymbol{n}, r) = \frac{2a^2}{M^{(i)}}\rho r\left(1-n_i^2\right)^{1/2} E(\boldsymbol{n})f(r) \tag{25}$$

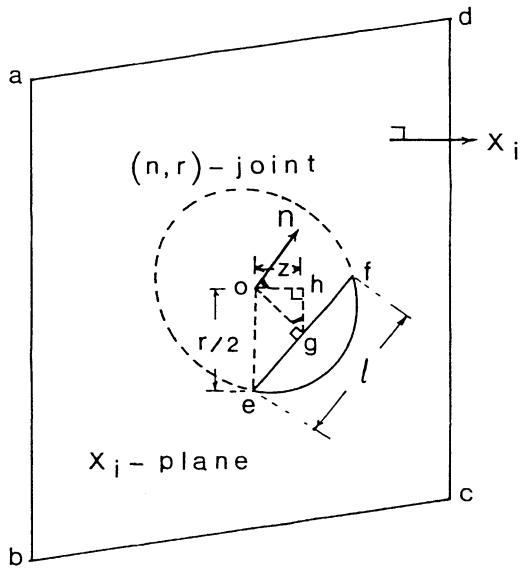

Fig. 5. Relation between trace length l(ef) on x_i-plane and distance z(oh) of center of ($\boldsymbol{n}$, r)-joint from the plane.

This equation is useful because the density function $E^{(i)}(\boldsymbol{n}, r)$ defined on a plane is expressed by the functions $E(\boldsymbol{n})$ and $f(r)$ defined in the related volume.

4.3 Trace length

Let us consider again the ($\boldsymbol{n}$, r)-joints visible on the x_i-plane. From Fig. 5, it becomes clear that the trace length l of an ($\boldsymbol{n}$, r)-joint must satisfy the following relation (see also Warburton, 1980);

$$l = \left[r^2 - \frac{4z^2}{\left(1 - n_i^2\right)} \right]^{1/2} \tag{26}$$

Since we are now thinking of only the ($\boldsymbol{n}$, r)-joints, n_i and r in the equation can be considered constant. Differentiating Eq. (26) leads to

$$-\delta z = \left(1 / 4z\right)\left(1 - n_i^2\right) l \delta l \tag{27}$$

where the minus sign means that an increase of l leads to decrease of z.

Within all $(\boldsymbol{n}, r)$-joints visible on the x_i-plane, only the joints having their centers at a distance of z to $z+(-\delta z)$ from the x_i-plane give trace lengths ranging from l to $l+\delta l$. In other words, the centers of the $(\boldsymbol{n}, r)$-joints must be placed inside the volume $2a^2(-\delta z)$ to give their trace lengths ranging from l to $l+\delta l$. Let $P^{(i)}$ be the ratio of the number of the $(\boldsymbol{n}, r)$-joints making trace lengths from l to $l+dl$ to the number of all $(\boldsymbol{n}, r)$-joints. To make traces with x_i-plane, the centers of $(\boldsymbol{n}, r)$-joints must be placed inside the volume $a^2r(1-n_i^2)^{1/2}$. Then the ratio $P^{(i)}$ is given by

$$P^{(i)} = \frac{2a^2(-\delta z)}{a^2 r\left(1-n_i^2\right)^{1/2}} \tag{28}$$

Using Eq. (27), $P^{(i)}$ can be rewritten as

$$P^{(i)} = \frac{l\delta l}{r\left(r^2-l^2\right)^{1/2}} \tag{29}$$

Remember that $M^{(i)}E^{(i)}(\boldsymbol{n}, r)d\Omega dr$ equals the estimated number of all $(\boldsymbol{n}, r)$-joints which intersect the x_i-plane. So, multiplying it by $P^{(i)}$ leads to the number of the $(\boldsymbol{n}, r)$-joints giving trace lengths from l to $l+\delta l$ visible on the x_i-plane. In order to get the total number of all visible joints giving the same trace length, $M^{(i)}P^{(i)}E^{(i)}(\boldsymbol{n}, r)d\Omega dr$ must be integrated over $\Omega/2$ and $l \le r < \infty$. Then we have

$$M^{(i)}\int_l^\infty \int_{\Omega/2} P^{(i)}E^{(i)}(\boldsymbol{n}, r)d\Omega dr = M^{(i)}\Phi^{(i)}(l)\delta l \tag{30}$$

where a new density function $\Phi^{(i)}(l)$ is used to show the statistical distribution of the trace lengths on the x_i-plane. The range of integration with respect to r is taken to be from l to ∞. This is because any joint cannot make the trace length of l if its diameter r is less than l.

Using Eqs. (24), (25) and (29) in Eq. (30), we finally have

$$\begin{aligned}\Phi^{(i)}(l) &= \frac{2a^2\rho}{M^{(i)}}\int_{\Omega/2}\left(1-n_i^2\right)^{1/2}E(\boldsymbol{n})d\Omega\int_l^\infty \frac{l}{\left(r^2-l^2\right)^{1/2}}f(r)dr \\ &= \frac{1}{\left(\langle r\rangle\right)}\int_l^\infty \frac{l}{\left(r^2-l^2\right)^{1/2}}f(r)dr\end{aligned} \tag{31}$$

Note that the right side of the equation does not include any information on the

orientation of the observed plane (=x_i-plane). In other words, $\Phi^{(i)}(l)$ yields the same function regardless of the orientation of observed planes. Accordingly, the superscript (i) in $\Phi^{(i)}(l)$ can be omitted. Equation (31) is well known as Abel's equation satisfying the following relation (Kendall and Moran, 1963):

$$\langle l^n \rangle = \frac{\langle r^{n+1} \rangle}{\langle r \rangle} \int_0^{\pi/2} \sin^{n+1}\theta d\theta \tag{32}$$

where

$$\langle l^n \rangle = \int_0^\infty l^n \Phi(l) dl \tag{33}$$

$$\langle r^n \rangle = \int_0^\infty r^n f(r) dr \tag{34}$$

Using Eqs. (20) and (32), the terms $<r^3>$ and ρ in Eqs. (10) and (11) can be rewritten in terms of $m^{(L)}/h$ and $<l^n>$ which are all measurable quantities in situ. Finally, the second-rank crack tensor, for example, is given by

$$F_{ij} = \frac{3\pi}{8} \frac{\langle l^2 \rangle}{\langle l \rangle} \frac{m^{(L)}}{h \langle |\boldsymbol{n} \cdot \boldsymbol{q}| \rangle} N_{ij} \tag{35}$$

where N_{ij} is a tensor depending only on the joint orientation (see Eq. (4)).

When using Eq. (35), the determination of the trace lengths is most difficult. It is rather a rare case to have such large excavated walls (or cliffs) on which we can determine the trace lengths. To avoid this difficulty, another approach must be searched for. Fortunately, there are many possibilities if an additional assumption is allowed to be made. For example, the function $f(r)$ is assumed to be given by Eq. (3). Then, the moments of l in Eq. (35), i.e.$<1>$ and $<l^2>$, can be replaced by the number of joints visible on unit area of an excavated wall (Oda, 1984). Counting the number is much easier than measuring the trace lengths.

5. An Example

In order to exemplify the detailed procedure leading to the determination of crack tensor, a typical site is chosen to investigate. (Here, only the second rank tensor is calculated. Note, however, that no difficulty arises in the calculation of higher rank tensors.) The site, located near Nakatsugawa, Central Japan, is composed of moderately jointed, fresh granite. Joints were surveyed with the

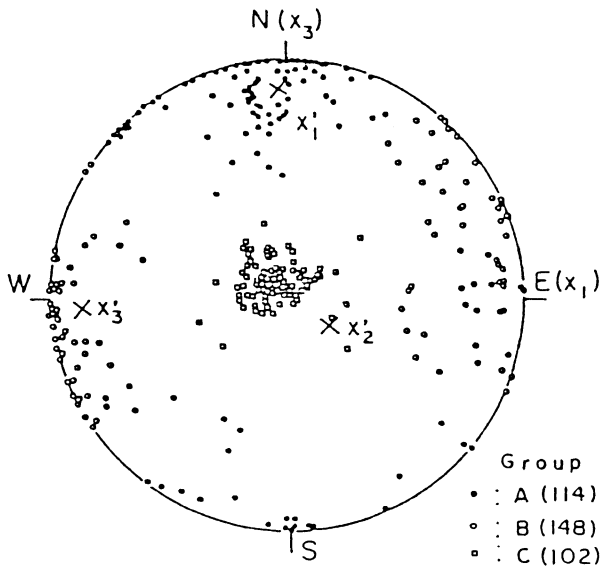

Fig. 6. Schmidt's equal area projection of poles normal to joints (lower hemisphere), together with the principal axes of F_{ij}.

special emphasis on the following points:

Orientation of joints: Three orthogonal scanning lines (EW, NS and vertical) were set on the surface of the granite (25 m × 20 m × 7 m). Strike and dip were measured whenever the scanning lines cross a joint. Orientation of joints is shown by plotting their normals as poles on Schmidt' equal area net (Fig. 6). In regard to Fig. 6, all joints were classified into three groups ((A), (B) and (C)). The density function $E(\boldsymbol{n})$ for each group is shown separately in Fig. 7. Using the data of Fig. 7 in Eq. (4), $N_{ij}^{(A)}$, $N_i^{(B)}$, and $N_{ij}^{(C)}$ are calculated as follows:

$$N_{ij}^{(A)} = \begin{pmatrix} N_{11} & N_{12} & N_{13} \\ N_{21} & N_{22} & N_{33} \\ N_{31} & N_{32} & N_{33} \end{pmatrix} = \begin{pmatrix} 0.135 & -0.010 & -0.041 \\ -0.010 & 0.071 & 0.078 \\ -0.041 & 0.078 & 0.794 \end{pmatrix} \tag{36}$$

$$N_{ij}^{(B)} = \begin{pmatrix} 0.789 & 0.049 & 0.123 \\ 0.049 & 0.058 & 0.011 \\ 0.123 & 0.011 & 0.153 \end{pmatrix} \tag{37}$$

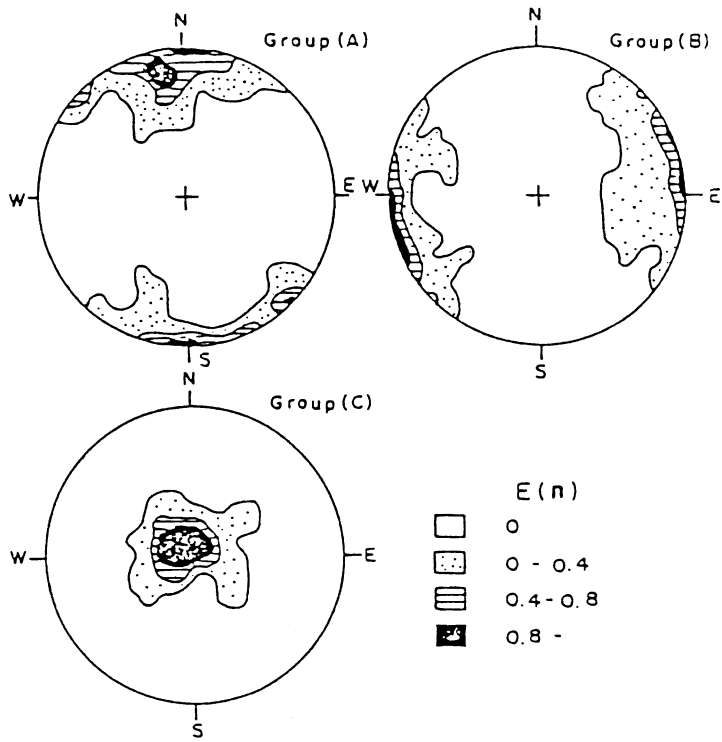

Fig. 7. Density function $E(\boldsymbol{n})$ for each joint group.

$$N_{ij}^{(C)} = \begin{pmatrix} 0.031 & -0.067 & -0.003 \\ -0.067 & 0.994 & 0.080 \\ -0.003 & 0.080 & 0.025 \end{pmatrix} \tag{38}$$

In the calculation, we referred to the axes x_1, x_2 and x_3 given in Fig. 7.

Trace lengths of points: Joint traces, which were visible on the horizontal section (25 m × 20 m), were carefully mapped (Fig. 8). Two kinds of data were prepared using the map of the joint traces for each group separately: First a scanning line pointing to a direction $\boldsymbol{q}$ was set. The number of cracks crossed by the scanning line was counted to give $m^{(L)}/h$, and the correction term $<|\boldsymbol{n}\cdot\boldsymbol{q}|>$ was also calculated by using the density function of Fig. 7. Several trials have proved that $(m^{(L)}/|h|<|\boldsymbol{n}\cdot\boldsymbol{q}|>)$ remains almost constant, not depending much on the selected direction $\boldsymbol{q}$ of the scanning line. Secondly, the frequency histograms of the trace lengths were prepared (Fig. 9). The joints belonging to gtoup (C) do not appear on the horizontal

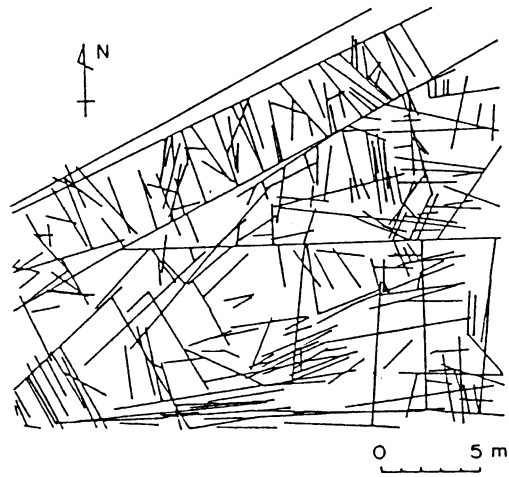

Fig. 8. Map showing the joint traces on a horizontal section.

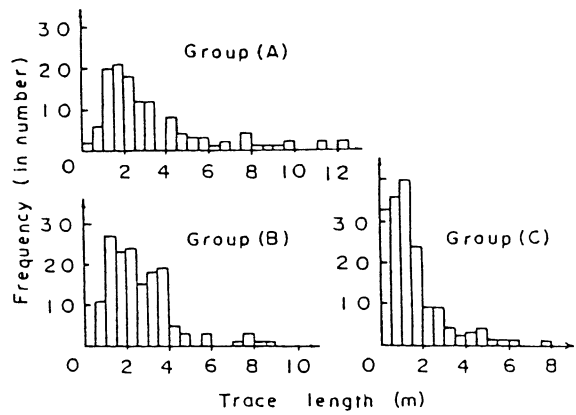

Fig. 9. Histograms of the trace lengths. (Four more joints having 13.9 m, 21.0 m, 23.7 m and 28.8 m in trace length must be added to the diagram for group (A).)

map because they are subparallel to the observed plane. So, two large vertical cliffs located near the horizontal section were carefully skeched to provide a corresponding histogram (Fig. 9). These histograms are similar in the shape, but differ in the mean and standard deviation. This is the main reason that the joints were classified into the three groups. Using these diagrams, the moments of the trace length, $<l>$ and $<l^2>$, were calculated.

Using all these data in Eq. (35), the crack tensors $F_{ij}^{(A)}$, $F_{ij}^{(B)}$ and $F_{ij}^{(C)}$ for the

groups (A), (B) and (C) were separately calculated, and were summed up to give the final crack tensor F_{ij}; as follows:

$$F_{if} = \begin{pmatrix} 9.965 & 0.162 & 1.651 \\ 0.162 & 5.091 & 1.066 \\ 1.651 & 1.066 & 7.715 \end{pmatrix} \tag{39}$$

If the reference axes are selected as the principal axes x_1', x_2' and x_3' of the crack tensor, then Eq. (39) becomes

$$F_{ij} = \begin{pmatrix} 10.919 & 0 & 0 \\ 0 & 7.282 & 0 \\ 0 & 0 & 5.169 \end{pmatrix} \tag{40}$$

with the principal axes plotted on Fig. 6.

REFERENCES

Kachanov, M. (1980), Continuum model of medium with cracks, J. Eng. Mech. Div. Am. Soc. Civ. Engrs., **106** (EM5), 1039–1051.

Kanatani, K. (1984), Distribution of directional data and fabric tensors, Int. J. Eng. Sci., **22(2)**, 149–164.

Kawamoto, T., Ichikawa, Y., and Kyoya, T. (1986), Deformation and fracturing behavior of discontinuous rock mass and damage mechanics theory, Int. J. Numer. Analy. Methods Geomech., **12**, 1–30.

Kendall, M. G. and Moran, P. A. P. (1963), Geometrical Probability, p. 87. Hafner, New York.

Oda, M. (1983), A method for evaluating the effect of crack geometry on the mechanical behavior of cracked rock masses, Mechanics of Materials, **2**, 163–171.

Oda, M. (1984), Similarity rule of crack geometry in statistically homogeneous rock masses, Mechanics of Materials, **3**, 119–129.

Oda, M. (1985), Permeability tensor for discontinuous rock masses, Geotechnique, **35(4)**, 483–495.

Oda, M. (1988), An experimental study of the elasticity of mylonite rock with random cracks, Int. J. Rock Mech. Min. Sci. & Geomech. Abstr., **25(2)**, 59–69.

Oda, M., Yamabe, T., and Kamemura, K. (1986), A crack tensor and its relation to wave velocity anisotropy in jointed rock masses, Int. J. Rock Mech. Min. Sci. & Geomech. Abstr., **23(6)**, 387–397.

Oda, M., Hatsuyama, Y., and Ohnishi, Y (1987), Numerical experiments of permeability tensor and its application to jointed granite at Stripa mine, Sweden. J. geophys. Res., **92(B8)**, 8037–8048.

Roulean, A. and Gale, J. E. (1985), Statistical characterization of the fracture system in the Stripa granite, Sweden, Int. J. Rock Mech. Min. Sci. & Geomech. Abstr., **22(6)**, 353–367.

Satake, M. (1983), Fundamental quantities in the graph approach to granular materials. Mechanics of Granular Materials, New Models and Constitutive Relations, edited by Jenkins, J. T. and Satake, M., pp. 9–19, Elsevier, New York.

Warburton, P. M. (1980), A stereological interpretation of joint trace data, Int. J. Rock Mech. Min. Sci. & Geomech. Abstr., **17**, 181–190.